Design and Simulation of Solar PV DC Microgrid for Rural Electrification

Vipul Narad[1], Prof.Bushra Khan[2]

PG[1] Student, Department of Electrical Engineering, AGPCE, Nagpur, MS-India
Guide[2], Department of Electrical Engineering, AGPCE, Nagpur, MS-India

Abstract: *In this paper We present the analysis and design of the e dc microgrid system for electrification. The microgrid configuration has been driven by field information gathered from India. The important parameter of such system depends on the Microgrid capacity of the transmission network which overflows the value of the voltage and the current from the main grid, which power the cost matrix analysis of the overall system which has to be equal. In this paper, we compute that the excessive cost of power (COE) for the proposed dc microgrid framework will be under minimal charges as put forth by the electrification governing agency according to the per kW-hr. We additionally present test results from a privately introduced dc microgrid model that exhibit the consistent state conduct, the bother reaction, and the general efficiency of the framework. The results show the reasonableness of the introduced dc microgrid design has totally inflicts with the main grid feasibly and found out to be very easy to implement without any extra cost to the system as far as the rising districts and the number of population in such districts are concerns.*

I.   Introduction

There are at present 1.3 billion individuals in rustic creating locales without access to power [1]. This number is anticipated to increment in spite of expanded network tied age since there is as yet a significant control deficit in urban territories [1]– [3]. Microgrids have been seen as a reasonable choice to give power to country zones where the expense of framework expansion is restrictive [4], [5]. As of late, the falling expense of sun based vitality has started expanding enthusiasm for creating sustainable techniques for country electrification [6]– [8]. In any case, battery costs have not declined at indistinguishable rate from sun based photovoltaic (PV) boards. Since the dominating private use is amid evening time hours [9], the expense of put away power use is a key figure of legitimacy. In such manner, dc microgrids have exhibited guarantee as a suitable technique for empowering enhanced efficiency and versatility for off-network frameworks [8]– [13]. In this paper, we present and tentatively exhibit a dc microgrid design that gives an adaptable answer for country electrification. We ascertain the levelized cost of power (LCOE) of the depicted engineering dependent on BOM expenses of the proposed framework and field overviews did by research accomplices. We present an equipment model setup used to exhibit the consistent state conduct and the irritation reaction of the proposed engineering. This rest of the paper is sorted out as pursues. Sec-tion II exhibits a diagram of the dc microgrid framework topology, the circulated control execution, and LCOE counts. Area III exhibits a downsized PV-based microgrid model used to tentatively show the task and steadiness of the framework. Segment IV finishes up the paper.

This remainder of the paper is organized as follows. Sec- tion II presents an overview of the dc microgrid system topology, the distributed control implementation, and LCOE calculations. Section III presents a scaled-down PV-based microgrid prototype used to experimentally demonstrate the operation and stability of the system. Section IV concludes the paper.

II.   System Overview And Implementation

In this area, we present a diagram of the dc microgrid framework design and do a cost examination to get the LCOE of the proposed microgrid over a multi year skyline. Moreover, we present a model equipment usage used to tentatively approve the activity and steadiness of the framework..

A. *Overview of architecture*

A review of the dc microgrid engineering is appeared in Fig. 1. The key parts of the framework are 1) the most extreme power point following (MPPT) source converter, 2) the fanout hubs, and

3)   the family unit control the executives units (PMUs). An ostensible appropriation voltage somewhere in the range of 360 and 400 V is utilized to keep line misfortunes unobtrusive while conforming to the developing norms for dc influence [14]. The decision additionally empowers utilization of promptly accessible 600 V control semiconductor gadgets. The matrix voltage is changed over to 12 V at the family units for capacity and machine use. The MPPT source converter is in charge of working the sun oriented boards at the

pinnacle control point just as identifying and detaching flaws on the matrix. The fanout hubs total utilization from a neighborhood bunch of houses (3-5 family units inside a 15 m range) and switch and meter the use of individual families associated with the line. This usefulness discourages burglary of intensity and segregates blames on the matrix. Additionally each fanout hub consolidates a fixed proportion 8:1 dc transport converter. The transport converters, which have an appraised efficiency of 95%, are financially made gadgets normally utilized in server farm applications [15]. They likewise give galvanic segregation to the associated family units which is an essential security thought. The fanout hub gives a middle (45-50 V) transport to the nearby bunch of houses. Since the fanout hubs utilize a fixed proportion converter, the data understood in the framework voltage level is protected and passed on to the family units downstream. At long last, every family unit interfaces to the microgrid through a family unit control the board unit (PMU), which changes over the 45-50 V fanout transport voltage to 12 V through a buck converter for all family unit apparatuses, and furthermore incorporates battery stockpiling. What's more, the
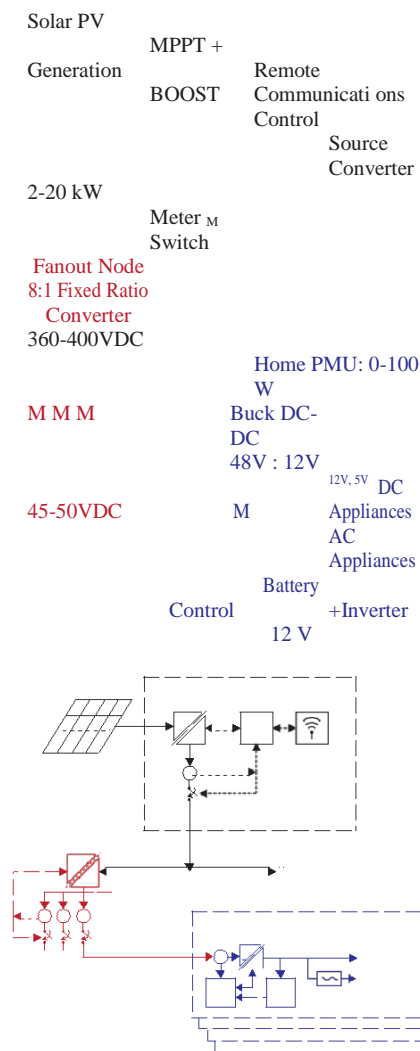
PMUs can carefully convey data

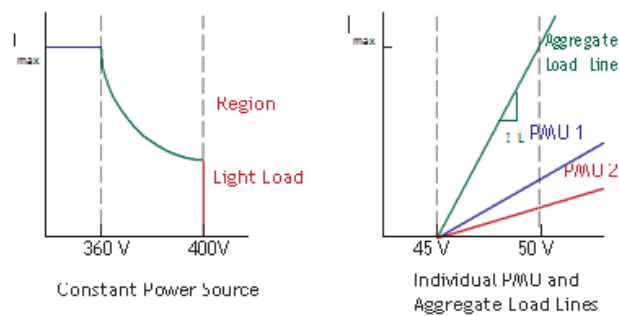**Fig. 1.** An architectural overview of the dc microgrid system.

Fig. 2. Source and load impedances. The PMU load-line slope and offset are controllable variables.

or example, value, charge-condition of family units, credits, and use both locally to the end-client and remotely to the framework administrator.

A notable property of the dc microgrid design is the appropriated control of the network voltage, which empowers both prompt power sharing and a measurement for deciding the accessible lattice control. A hang voltage control sharing plan is actualized, as appeared in Fig. 2, wherein the transport voltage hangs in light of low-supply/intense interest. This hang profile is a consequence of a consistent power source which is framed when a MPPT converter is associated with a sun powered PV board. The PMUs have a controllable utilization profile (load-line) that can decrease control drawn from the lattice by utilizing privately put away vitality for the battery to control associated family unit loads. Changing converters directed to execute a heap line profile have been appeared to have the properties of both substantial scale and steady detachment [8]. Interconnected systems of latent converters have been appeared to be steady utilizing vitality based (Lyapunov) strategies].

B. Furthermore, the engineering of the dc microgrid plans to limit the misfortunes related with put away vitality. Since capacity is circulated to the individual family unit PMUs, the quantity of change steps and line misfortunes are diminished. Appropriated stockpiling gives solid arrangement of power day in and day out and furthermore takes into consideration family loads to be decoupled from the network supply when required. Moreover, family unit responsibility for empowers flexible, request driven development of capacity in the network, since every family settles on choices about the extent of the put away supply dependent on wanted evening time utilization.*Levelized Cost of Electricity Calculations*

The levelized cost of electricity (LCOE) is calculated based on the specifications shown in Table II. Cost assumptions of Fanout Nodes and PMUs were based on BOM costs of components used in the prototype system at low production volumes (500 units). A 15 year time horizon was used based on rated lifetimes of solar panels and the power converter com-ponents. Lithium Iron Phosphate (LFP) batteries were used to calculated storage costs due to having a favorable combination of longer cycle life and higher safety in comparison to other

lithium-ion chemistries [17]. Over a 15 year window it is assumed that the LFP batteries would have to be replaced twice with an estimated cycle life of greater than 2000 cycles without significant loss of capacity [18]. Wiring costs were estimated based on using aluminum distribution wire sized at keeping voltage drop across 1 km under 3% at full load. The calculated LCOE of the dc microgrid is favorable in comparison to presently deployed solar microgrid systems and also with grid power rates on certain Hawaiian islands [19].

C. Prototype implementation

III. So as to tentatively approve the proposed dc small scale matrix engineering, a downsized 400 W equipment model setup, appeared in Fig. 3a, was developed and introduced at the University of California, Berkeley. The full specifications and appraisals for the model setup are exhibited in Table I.

IV. The converter plans and walled in areas are appeared in Fig. 3. The MPPT source converter (Fig. 3b) comprises of a 2-stage interleaved lift converter, combine assurance, and connectors for PV information and transport yield. The fanout hub is executed utilizing an industrially accessible 8:1 fixed proportion 300 W dc converter which changes over from 360-400 V to 45-50 V. The family unit PMU (Fig. 3c) comprises of a 100 W synchronous buck converter, combine security, 100 W-hrs of battery stockpiling, and connectors for 45-50 V transport info and 12 V dc yield. The heap line is executed utilizing corresponding criticism of voltage at the info terminal of the converter as appeared in Fig. 4. The yield from the external voltage circle shapes the reference to the internal current circle. The increase of the external circle decides slant of the heap line (input impedance) of the converter. Accomplishing load-line direction through such a corresponding criticism plot has been utilized for yield control of dc-dc converters [20], [21]. We utilize similar procedures to accomplish load-line direction on the contribution of the PMU buck converters

III. Experimental Results

In this section, we present experimental results that demon-strate the operation of the dc microgrid prototype setup under various operating conditions. The steady state behavior of the PMU converters, and the perturbation response of grid voltage are shown as the power from the source is varied. The startup

TABLE I
SPECIFICATIONS AND RATINGS FOR PROTOTYPE MICROGRID

Solar PV array	
Rated power	400 W
Rated open circuit voltage	200 V
MPPT Source Converter	
Topology	2-phase boost converter
Rated power	400 W
Rated output voltage	400 V
Switching frequency	100 kHz
Household PMU	
Topology	Synchronous Buck
Rated power	100 W
Rated output voltage	12 V
Switching frequency	250 kHz

TABLE II
LCOE PARAMETERS AND CALCULATION OVER A 15 YEAR HORIZON

System Parameters	
Number of Households	100
Daily Usage	100 W-hrs/day
Radius of Microgrid	1 km
Generation Costs	
Rated Size of Solar Panels	2 kW
Cost of Solar Panels	$0.70 per W
Cost of Source Converter	$0.25 per W
Total Cost of Generation	$1,900
Fanout Node Costs	
No. of Fanout nodes in system	30
Cost of Fanout nodes	$0.20 per W
Total cost of Fanout nodes	$2,000
PMU Costs	
Power rating of individual PMU	100 W
Cost of PMUs	$0.15 per W
Total Cost of PMUs	$1,500
Battery Costs	
Storage per household	100 W-hrs
LFP Battery Cost	$0.50 per W-hr
Total Battery Costs over 15 years	$10,000
Wiring Costs	
Total T&D wiring costs	$4,000
Total System Cost	$19,400
LCOE of elec. delivered over 15 years	$0.35 per kW-hr

and shutdown behaviors of the various components of the grid are also shown.

A. *Experimental Test Setup*

A sunlight based board associated with a MPPT converter carries on as a consistent power source. So as to make a controllable steady power-hotspot for the examinations in this segment, a lift converter working in information current-control mode was utilized, i.e., where the information current from the voltage source is controlled. A schematic of the setup is appeared in Fig. 5. The info capacity to the framework can be differed by either by changing the information voltage to the current-controlled lift or by changing the present direction. An adjustment in the present direction was utilized to cause step changes in network control.*Steady State Behavior*

Fig. 6 shows the steady-state response of the PMU input current as a function of the grid voltage. The efficiencies of the Fanout and PMU converters used in the experiment setup

Fig A The scaled-down dc microgrid prototype used for ex-perimental validation.

are shown in Fig. 7. Both simulation and experimental results show the same relationship between current drawn by the PMU and input voltage. As shown, the current drawn by each PMU increases as the grid voltage increases, thus exhibiting a positive impedance characteristic. The slope of this load-line is fully programmable and set by the feedback gain of input voltage. The gain on the controller is set to achieve an input impedance of $Z = 2\ \Omega$. Once the PMU converter is operating in continuous conduction mode, both the simulation and experiment show that the steady state input impedance is $2\ \Omega$. When the converter is in discontinuous conduction mode, the input impedance is higher than idealized case. However,
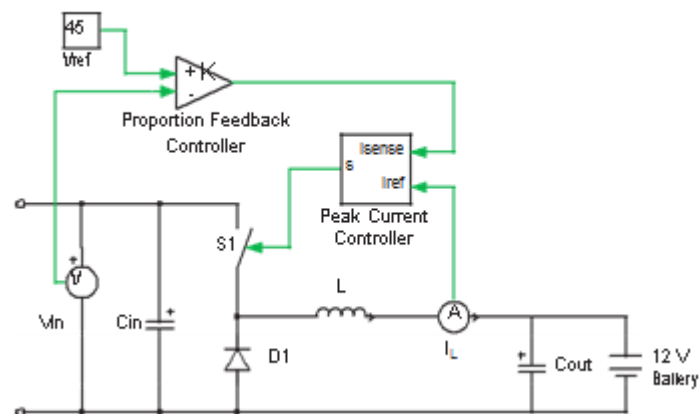

Fig. 4. PMU Load-line Implementation. The gain of the outer voltage loop sets the load-line slope.
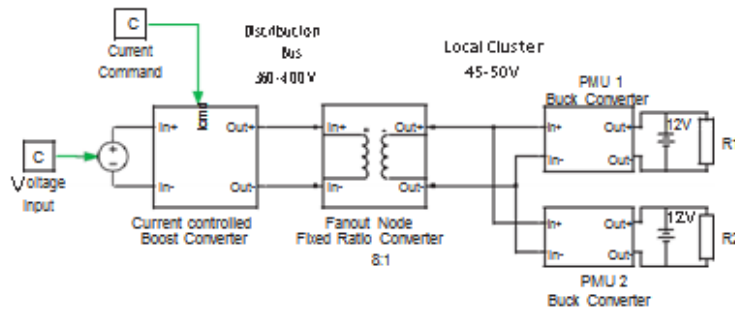
Fig. 5. Schematic of Experimental Setup.

this deviation does not have any significant impact on system behavior as will be shown by the perturbation response.

B . Response

Fig. 8 shows the perturbation response of the grid voltage, fanout hub voltage, and the information current to the 2 PMUs because of a stage change in the accessible lattice control. At first, the info capacity to the matrix is 5 W. At this dimension, the fanout hub is controlled on, yet the fanout transport voltage is underneath 45 V so the PMUs are not drawing any current from the framework; the power is dispersed in the fanout hub transport converter. At t = 0.19 s, the accessible matrix control is momentarily expanded from 5 W to 70 W by directing a stage change in information current drawn by the lift converter in the exploratory setup (Fig. 5). Promptly, the lattice voltage begins to rise, yet stays inside the 360 to 400 V run. This adjustment is because of the reaction of the PMUs, which increment their present attract reaction to the expansion in matrix voltage..

C   Behavior

Fig. 9a demonstrates the startup conduct of the microgrid. After the power source is turned on, the voltage on high voltage transport of the lattice begins to rise. The high voltage transport ascends to 400 V before the fanout hub begins to work. Upon turn on of the fanout hub BCM, t = 1 sec, the voltage on the fanout hub transport quickly ascends to 50 V. The underlying spike in PMU current is because of the info capacitors charging from 0 to 50 V. The PMUs associated with the fanout hub begin to draw current from the fanout transport as per their heap line.
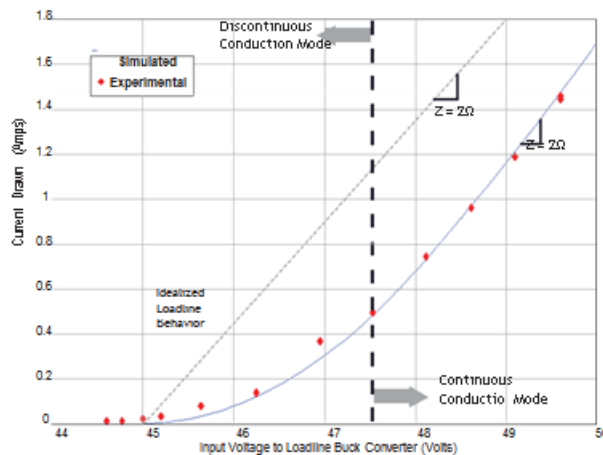

Fig. 6. Simulation and experimental results showing the change in input current of a PMU buck converter implementing a load-line profile in response to grid voltage on the fanout node bus.
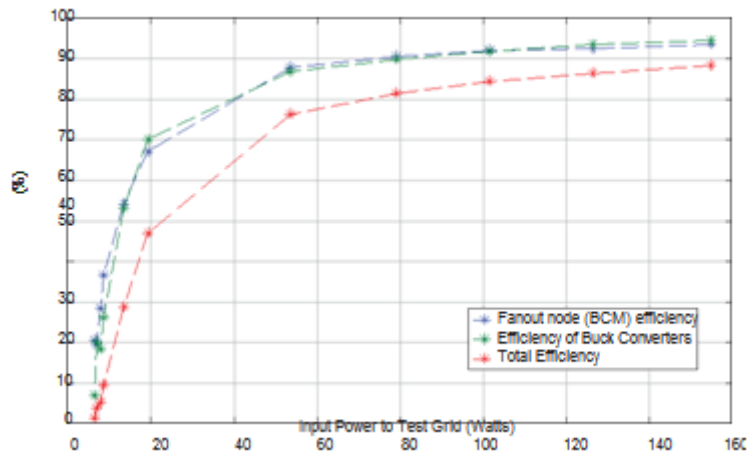
Fig. 7. Efficiency of the Fanout Bus Converter and PMU Buck converters as a function of input power for the configuration shown in Fig. 5.

This subsequently causes the voltage on both busses to droop and settle at an operating point determined by the available power and the slope of the aggregate PMU load-line.

Fig. 9b shows the shutdown behavior of the microgrid. As the bus voltages start to drop, the PMUs respond by drawing less current from the grid. Once the fanout bus voltage drops below 45 V, the PMUs do not draw any more current. As the grid voltage drops below 300 V the bus converter in the fanout nodes also shuts down and the grid voltage continues to fall. In both startup and shutdown scenarios, the household load on the low-voltage side of the PMU is decoupled due to the battery.

IV. Conclusions

This paper presented the Concept Design and implementation of a scalable dc microgrid architecture for rural electrification.
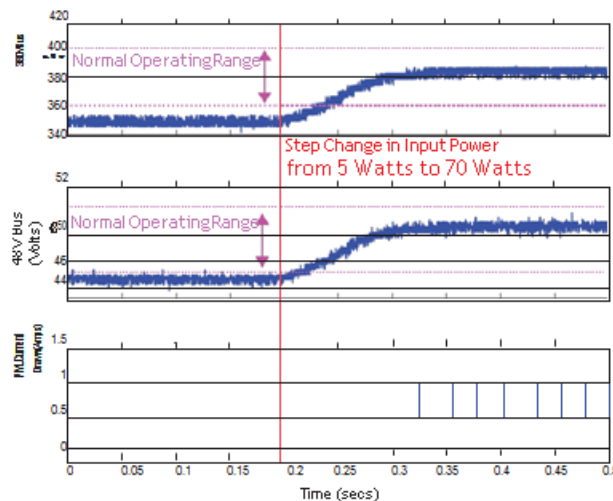

Fig. 8. Transient behavior of bus voltages and PMU current draw in response to a step increase in grid power (5 W to 70 W) at time $t = .19$ secs.

We experimentally demonstrated the operation and stability of the dc microgrid with distributed voltage control. The load-line control scheme implemented by the PMUs enables inte-gration of completely variable sources and requires minimal regulation overhead. Relative ratios of load-lines determine the power-sharing between the different PMUs, thereby allowing for load prioritization.

The dc microgrid described in this paper allows for maxi-mizing efficiency of stored electricity, a key figure of merit for off-grid system. The architecture shows promise in addressing the economic and technical challenges of electrifying rural emerging regions.

References

[1]. "Energy for all: financing access for the poor," tech. rep., IEA World Energy Outlook, 2011.
[2]. L. Srivastava and I. H. Rehman, "Energy for sustainable development inIndia: Linkages and strategic direction," *Energy Policy*, vol. 34, pp. 643– 654, Mar. 2006.
[3]. M. Nouni, S. Mullick, and T. Kandpal, "Providing electricity access to remote areas in India: An approach towards identifying potential areas for decentralized electricity supply," *Renewable & Sustainable Energy Reviews*, vol. 12, pp. 1187–1220, June 2008.
[4]. Z. Ding, M. Liu, W.-J. Lee, and D. Wetz, "An autonomous operation microgrid for rural electrification," in *2013 IEEE Industry Applications Society Annual Meeting*, pp. 1–8, IEEE, Oct. 2013.
[5]. T. Levin and V. M. Thomas, "Least-cost network evaluation of central-ized and decentralized contributions to global electrification," *Energy Policy*, vol. 41, pp. 286–302, Feb. 2012.
[6]. S. C. Bhattacharyya, "Review of alternative methodologies for analysing off-grid electricity supply," *Renewable and Sustainable Energy Reviews*,vol. 16, pp. 677–694, Jan. 2012.
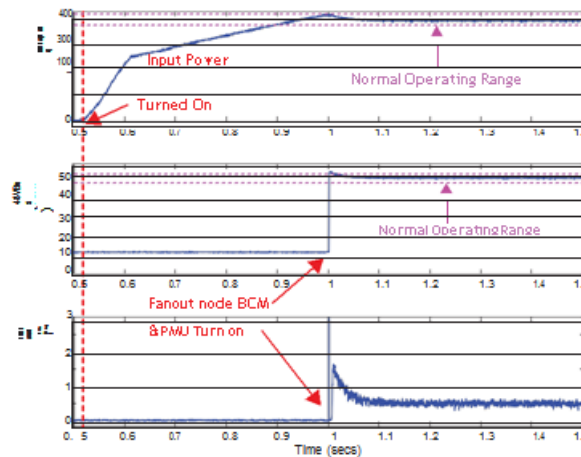
Startup behavior of experimental microgrid setup after input voltage source is turned on at time $t = .52$ secs. The available power from the source upon startup is 55 W
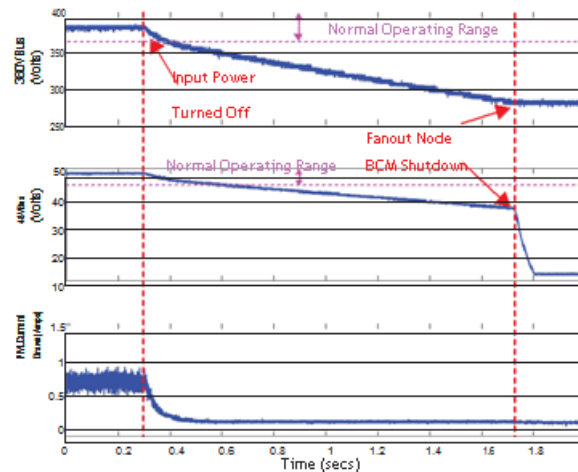
(b) Shutdown behavior of experimental microgrid setup after input voltage source is turned off at time $t = .3$ secs.

Fig. 9. Startup and shutdown behavior of prototype dc microgrid system with input power set to 55 W.

[7]. D. Soto, E. Adkins, M. Basinger, R. Menon, S. Rodriguez-Sanchez,
[8]. N. Owczarek, I. Willig, and V. Modi, "A prepaid architecture for solar electricity delivery in rural areas," in Proceedings of the Fifth Interna-tional Conference on Information and Communication Technologies and Development - ICTD '12, (New York, New York, USA), p. 130, ACM Press, Mar. 2012.
[9]. P. A. Madduri, J. Rosa, S. Sanders, E. Brewer, and M. Podolsky, "Design and verification of smart and scalable DC microgrids for emerging regions," 2013 IEEE Energy Conversion Congress and Exposition, pp. 73–79, Sept. 2013.

[10]. D. Soto and V. Modi, "Simulations of Efficiency Improvements Using Measured Microgrid Data," Global Humanitarian Technology Confer-ence (IGHTC), 2012 IEEE, pp. 369–374, 2012.

[11]. D. Boroyevich, I. Cvetkovic, D. Dong, R. Burgos, F. Wang, and F. Lee,

[12]. "Future electronic power distribution systems a contemplative view," in 2010 12th International Conference on Optimization of Electrical and Electronic Equipment, pp. 1369–1380, IEEE, May 2010.

[13]. W. Jiang and Y. Zhang, "Load Sharing Techniques in Hybrid Power Sys- tems for DC Micro-Grids," Power and Energy Engineering Conference (APPEEC), 2011 Asia-Pacific, pp. 1–4, 2011.

[14]. W. Zhang, D. Dong, I. Cvetkovic, F. Lee, and D. Boroyevich, "Lithium-based energy storage management for DC distributed renewable energy system," Energy Conversion Congress and Exposition (ECCE), 2011 IEEE, pp. 3270–3277, 2011.

[15]. L. Zhang, T. Wu, Y. Xing, K. Sun, and J. M. Gurrero, "Power control of DC microgrid using DC bus signaling," in 2011 Twenty-Sixth Annual IEEE Applied Power Electronics Conference and Exposition (APEC), pp. 1926–1932, IEEE, Mar. 2011.

[16]. "Emerge Alliance.," [Online] Available: http://www.emergealliance.org. "Vicor BCM Bus Converter Module," [Online] Available: http://www.vicorpower.com/dc-dc-converters-board-mount/bus-converter-module.

[17]. S. Sanders and G. C. Verghese, "Lyapunov-based control for switched power converters," Power Electronics, IEEE Transactions on, vol. 7, no. 1, pp. 17–24, 1992.
"A-123 Lithium Iron Phosphate Batteries.," [Online] Available: http://www.a123systems.com/lithium-iron-phosphate-battery.htm.

[18]. E. M. Krieger, J. Cannarella, and C. B. Arnold, "A comparison of lead-acid and lithium-based battery behavior and capacity fade in off-grid renewable charging applications," Energy, vol. 60, pp. 492–500, Oct. 2013. "Electric Rates for Hawaii Electric Light.," [Online] Available: http://www.hawaiielectriclight.com/helco/Residential-Services/Electric-Rates.

[19]. A. V. Peterchev and S. R. Sanders, "Load-Line Regulation With Estimated Load-Current Feedforward: Application to Microprocessor Voltage Regulators," Power Electronics, IEEE Transactions on, vol. 21, no. 6, pp. 1704–1717.

[20]. R. Redl and N. O. Sokal, "Near-Optimum Dynamic Regulation of DC-DC Converters Using Feed-Forward of Output Current and Input Voltage with Current-Mode Control," Power Electronics, IEEE Transactions on, no. 3, pp. 181–192, 1986.